# Two Series of Luminescent Flexible Polycarboxylate Lanthanide Coordination Complexes with Double Layer and Rectangle Metallomacrocycle Structures

**ARTICLE** *in* CRYSTAL GROWTH & DESIGN · JULY 2013

Impact Factor: 4.89 · DOI: 10.1021/cg400174r



**6 AUTHORS**, INCLUDING:

Guang-Feng Hou
Heilongjiang University
**170** PUBLICATIONS **749** CITATIONS

SEE PROFILE

Weizuo Li
Dalian University of Technology
**8** PUBLICATIONS **27** CITATIONS

SEE PROFILE

Guang-Ming Li
Heilongjiang University
**66** PUBLICATIONS **742** CITATIONS

SEE PROFILE

CRYSTAL GROWTH & DESIGN

Article

pubs.acs.org/crystal

# Two Series of Luminescent Flexible Polycarboxylate Lanthanide Coordination Complexes with Double Layer and Rectangle Metallomacrocycle Structures

Guang-Feng Hou, Hong-Xing Li, Wei-Zuo Li, Peng-Fei Yan,* Xiao-Hong Su, and Guang-Ming Li*

Key Laboratory of Functional Inorganic Material Chemistry (MOE), School of Chemistry and Materials Science, Heilongjiang University, Harbin 150080, P. R. China

Supporting Information

**ABSTRACT:** Two series of eight polycarboxylate lanthanide coordination complexes, namely, $[Ln(cpia)(H_2O)_2]\cdot 4H_2O$ {Ln = Ce (**1**), Nd (**2**), and Sm (**3**)} and $[Ln(cpia)(H_2O)_n]_2\cdot 2H_2O$ {Ln = Eu (**4**), Gd (**5**), Tb (**6**), Er (**7**), and Lu (**8**), $n$ = 5 in **4**−**7**; $n$ = 4 in **8**} {$H_3$cpia = *N*-[4-(carboxymethoxy)phenyl]iminodiacetic acid}, have been synthesized by self-assembly and characterized by IR, thermogravimetric analysis, and X-ray crystallography. Complexes **1**−**3** are isomorphic featuring two-dimensional double layer structures, while the isomorphic complexes **4**−**8** exhibit [2 + 2] rectangle metallomacrocycle structures. Further, photoluminescence (PL) spectra of complexes **2**, **4**, and **6** show the strong characteristic luminescence of Eu(III), Tb(III), and Nd(III) ions, respectively, suggesting that $cpia^{3-}$ is able to efficiently sensitize the luminescence of lanthanide ions.

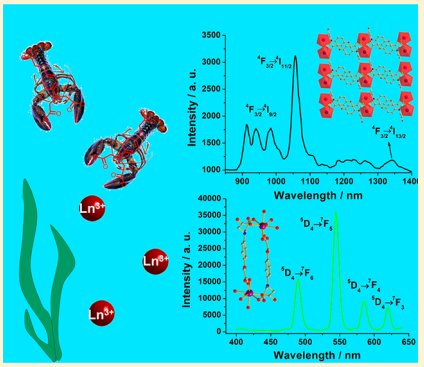


## INTRODUCTION

The design and synthesis of metal−organic complexes (MOCs) have attracted much attention due to their intrinsic physicochemical properties, which promote applications in the areas of luminescent materials, heterogeneous catalysis, magnetism, and electrochemistry, as well as their intriguing variety of architectures and topologies.[1−4] In this area, one important branch is the construction of lanthanide-based metal−organic complexes (LMOCs) because of many applications of such materials in biomedical and optical technologies.[5,6] It is well known that lanthanides ions have affinity for hard donor atoms, and thus the ligands containing oxygen atoms have been extensively used in the synthesis of lanthanide complexes. Several classes of ligands such as cryptands,[7] $\beta$-diketone,[8] and carboxylic acid[9] have been utilized. Among all types of ligands, polycarboxylate compounds with plentiful coordination points and varied coordination molds[10] represent a significant type of ligand for construction of new LMOC materials.[11] By designing the distances and angles between the carboxyls, chemists could control and synthesize multifariously novel structures.[12]

Accordingly, in the present work, we focus on synthesis of novel LMOCs by using the semirigid ligand, namely, *N*-[4-(carboxymethoxy)phenyl]iminodiacetic acid ($H_3$cpia), considering three reasons: (a) $H_3$cpia as a polycarboxylate compound possesses multiple coordination sites and can provide various coordination modes. (b) $H_3$cpia has not only the characteristics of flexibility and rigidity but also a long spacer, which will help to form amazing entangled or interpenetrated architectures. (c) The many O atoms and O−H groups of $H_3$cpia can serve as hydrogen bond acceptors as well as donors to construct supramolecular frameworks. The $H_3$cpia ligand was first reported in 2010,[13] in which the $H_3$cpia ligand reacted with a transition metal to produce four complexes with three-dimensional (3D) supramolecular networks. Herein, we report the synthesis, structure, and photoluminesce of two series of eight LMOCs, which represent the first example of $H_3$cpia-based LMOCs.

## EXPERIMENTAL SECTION

**Materials and Measurements.** All commercially available chemicals were reagent grade and used as received. $LnCl_3\cdot 6H_2O$ were synthesized by dissolving lanthanide oxide in a slight excess of hydrochloric acid. Elemental analyses of C, H, N were performed on a Perkin-Elmer 2400 elemental analyzer. The IR spectra were recorded on a Perkin-Elmer Spectrum 100 FT-IR spectrometer equipped with a DGTS detector (32 scans) by using KBr disks in the range of 4000 to 500 $cm^{-1}$. Thermal analyses were conducted on a Perkin-Elmer STA 6000 with a heating rate of 10 °C·$min^{-1}$ in a temperature range from 30 to 800 °C under air atmosphere. The luminescent spectra for the powdered solid samples were recorded at room temperature on an Edinburgh FLS 920 fluorescence spectrophotometer.

**Synthesis of *N*-[4-(Carboxymethoxy)phenyl]iminodiacetic Acid ($H_3$cpia).** The ligand $H_3$cpia was synthesized using an modified method described elsewhere.[14] A solution of KOH (22.40 g, 0.4 mol) in water (100 mL) was added dropwise to a solution of monochloroacetic acid (37.92 g, 0.4 mol) in water (100 mL). To the resulting alkaline solution, 4-amino-phenol (10.93 g, 0.1 mol) was added, and

Received: January 29, 2013
Revised: July 4, 2013
Published: July 8, 2013

   dx.doi.org/10.1021/cg400174r | Cryst. Growth Des. 2013, 13, 3374−3380

**Table 1. Crystal Data and Structure Refinements for Complexes 1−8**

| crystal parameters | 1 | 2 | 3 | 4 | 5 | 6 | 7 | 8 |
|---|---|---|---|---|---|---|---|---|
| empirical formula | $C_{12}H_{22}CeNO_{13}$ | $C_{12}H_{22}NdNO_{13}$ | $C_{12}H_{22}SmNO_{13}$ | $C_{24}H_{44}Eu_2N_2O_{26}$ | $C_{24}H_{44}Gd_2N_2O_{26}$ | $C_{24}H_{44}Tb_2N_2O_{26}$ | $C_{24}H_{44}Er_2N_2O_{26}$ | $C_{24}H_{40}Lu_2N_2O_{24}$ |
| formula weight | 528.43 | 532.55 | 538.66 | 1080.53 | 1091.11 | 1094.45 | 1111.13 | 1090.5 |
| crystal system | triclinic | triclinic | triclinic | monoclinic | monoclinic | monoclinic | monoclinic | monoclinic |
| space group | $P\bar{1}$ | $P\bar{1}$ | $P\bar{1}$ | $C/2c$ | $C/2c$ | $C/2c$ | $C/2c$ | $C/2c$ |
| $a$ (Å) | 9.4465(19) | 9.3836(19) | 9.3134(19) | 29.709(11) | 29.7113(8) | 29.689(6) | 29.692(6) | 29.373(1) |
| $b$ (Å) | 9.830(2) | 9.834(2) | 9.778(2) | 8.793(5) | 8.7956(2) | 8.7752(18) | 8.7398(17) | 8.7102(3) |
| $c$ (Å) | 11.903(2) | 11.888(2) | 11.839(2) | 14.599(7) | 14.6009(4) | 14.576(3) | 14.523(3) | 14.6315(8) |
| $\alpha$ (°) | 70.18(3) | 70.02(3) | 70.28(3) | 90 | 90 | 90 | 90 | 90 |
| $\beta$ (°) | 71.73(3) | 71.86(3) | 72.01(3) | 111.26(2) | 111.409 | 111.42(3) | 111.64(3) | 113.921(6) |
| $\gamma$ (°) | 67.28(3) | 67.37(3) | 67.68(3) | 90 | 90 | 90 | 90 | 90 |
| $V$ (Å$^3$) | 937.8(3) | 930.9(3) | 918.4(3) | 3554(3) | 3552.4(2) | 3534.9(12) | 3503.0(12) | 3421.9(3) |
| $Z$ | 2 | 2 | 2 | 4 | 4 | 4 | 4 | 4 |
| $D_{caled}$ (Mg cm$^{-3}$) | 1.871 | 1.900 | 1.948 | 2.019 | 2.040 | 2.056 | 2.107 | 2.117 |
| $\mu$ (mm$^{-1}$) | 2.494 | 2.856 | 3.265 | 3.600 | 3.805 | 4.072 | 4.863 | 5.835 |
| collected/unique | 9256/4266 | 9200/4220 | 9039/4183 | 16919/4062 | 9405/4077 | 16718/4044 | 16207/3989 | 7370/3905 |
| $R_{int}$ | 0.0246 | 0.241 | 0.0244 | 0.0249 | 0.0259 | 0.0217 | 0.0363 | 0.0254 |
| GOF on $F^2$ | 1.086 | 1.044 | 1.052 | 1.121 | 1.039 | 1.055 | 1.046 | 1.027 |
| $R$ ($I > 2\sigma(I)$) | $^aR_1$ = 0.0270 | $^aR_1$ = 0.0268 | $^aR_1$ = 0.0245 | $^aR_1$ = 0.0216 | $^aR_1$ = 0.0259 | $^aR_1$ = 0.0183 | $^aR_1$ = 0.0227 | $^aR_1$ = 0.0286 |
| | $^bwR_2$ = 0.0658 | $^bwR_2$ = 0.0658 | $^bwR_2$ = 0.0585 | $^bwR_2$ = 0.0437 | $^bwR_2$ = 0.0465 | $^bwR_2$ = 0.0413 | $^bwR_2$ = 0.0427 | $^bwR_2$ = 0.0575 |
| $R$ (all data) | $^aR_1$ = 0.0291 | $^aR_1$ = 0.0301 | $^aR_1$ = 0.0267 | $^aR_1$ = 0.0280 | $^aR_1$ = 0.0411 | $^aR_1$ = 0.0215 | $^aR_1$ = 0.0333 | $^aR_1$ = 0.0360 |
| | $^bwR_2$ = 0.0719 | $^bwR_2$ = 0.0672 | $^bwR_2$ = 0.0594 | $^bwR_2$ = 0.0453 | $^bwR_2$ = 0.0539 | $^bR_1$ = 0.0215 | $^bwR_2$ = 0.0455 | $^bwR_2$ = 0.0613 |

$^aR_1 = (\Sigma||F_o| - |F_c||)/\Sigma|F_o|$. $^bwR_2 = [\Sigma w(F_o^2 - F_c^2)^2/\Sigma w(F_o^2)^2]^{1/2}$.



dx.doi.org/10.1021/cg400174r | Cryst. Growth Des. 2013, 13, 3374−3380

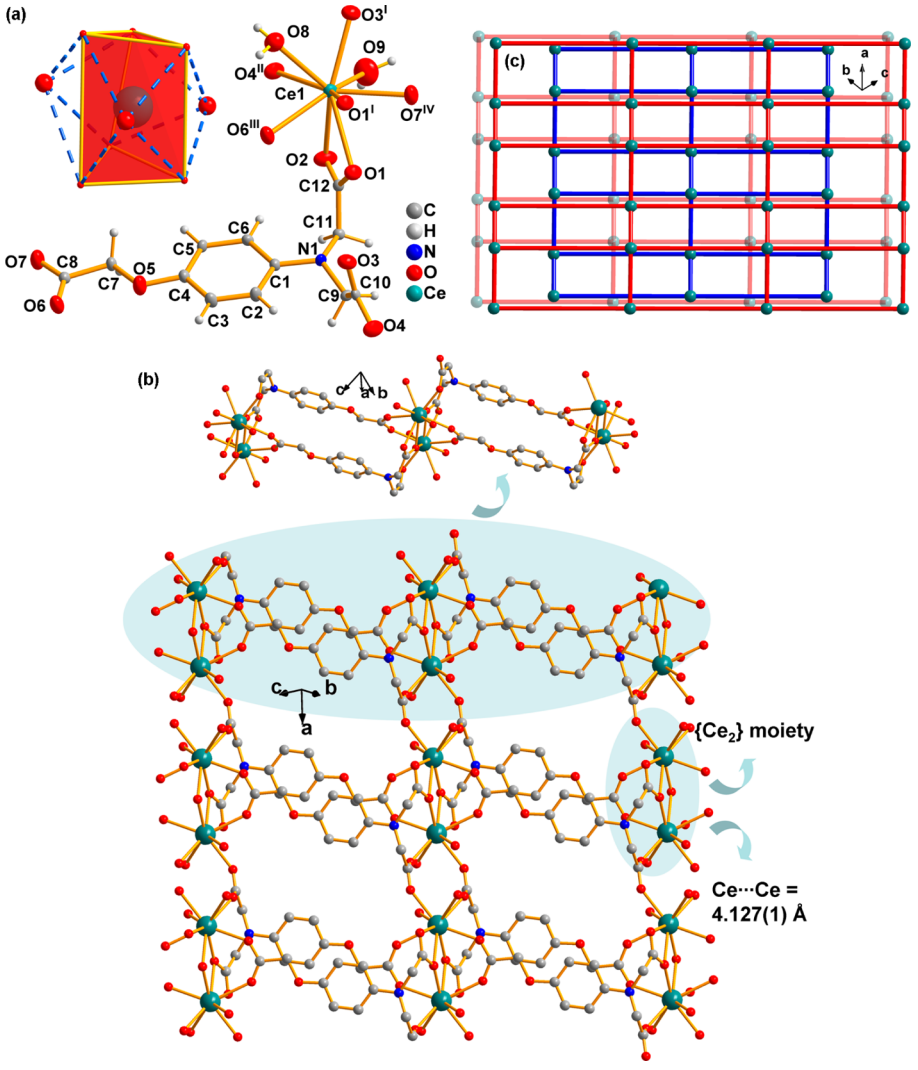


**Figure 1.** (a) Stick-ellipsoid representation of the asymmetric unit of complex **1** with thermal ellipsoids at 50% probability; lattice water molecules were omitted for clarity. The inset shows the coordination geometry of the Ce(III) center; (b) the double layer structure of complex **1**; (c) schematic illustration of A−B type stacking framework. Symmetry codes: (I) $1-x, 1-y, 2-z$; (II) $1+x, y, z$; (III) $1-x, 2-y, 1-z$; (IV) $x, -1+y, 1+z$.

the mixture was refluxed for 10 h at about 80 °C. Then the reaction mixture was cooled to room temperature, the pH value of the reaction mixture was carefully adjusted to about 2.0 with concentrated hydrochloric acid, and a pale brown precipitate appeared. The solid was filtered off and washed using 50 mL of cold deionized water, followed by vacuum drying to give $H_3$cpia in 74% yield based on 4-amino-phenol. $H_3$cpia was characterized by $^1$H NMR (500 MHz, DMSO): 3.93 (s, 4H), 4.51 (s, 2H), 6.35 (d, 2H), 6.76 (d, 2H), and the H atoms of the carboxylate groups were not observed. Elemental analysis calcd for $C_{12}H_{13}O_7N$ (283.2): C 50.89, H 4.63, N 39.54%; found: C 50.75, H 4.55, N 39.65%. IR (KBr pellet, cm$^{-1}$): 3394 (m), 2918 (w), 1740 (s), 1680 (s), 1510 (s), 1426 (m), 1359 (s), 1226 (m), 1132 (w), 1086 (m), 971 (w), 885 (w), 806 (m), 757 (m), 655 (w), 526 (w). UV−vis (MeOH, $\lambda_{max}$): 264, 320 nm.

**Synthesis of [Ce(cpia)(H$_2$O)$_2$]·4H$_2$O (1).** First, the $Na_3$(cpia) ligand was prepared by reacting $H_3$cpia (28.35 g, 0.1 mol) with NaOH (12.01 g, 0.3 mol) at a molar ratio of 1:3 in methanol solution. Three milliliters of water as a buffer layer was slowly diffused into a 15 mm ×150 mm test tube, which was already added to a solution of $CeCl_3·6(H_2O)$ (0.12 g, 0.33 mmol) in $H_2O$ (5 mL) and then 5 mL of $Na_3$(cpca) aqueous solution (0.8 mmol/mL) was added to the above mixture in the same way sequentially. Crystals suitable for X-ray determination were obtained in 2 days (28.8% yield based on Ce). Elemental analysis (%) calcd. for $C_{12}H_{22}CeNO_{13}$ (528.4): C 27.28, H 4.20, N 2.65%; found: C 27.40, H 4.04, N 2.67%. IR (KBr pellet, cm$^{-1}$): 3303 (s), 2921 (w), 1569 (s), 1512 (s), 1459 (s), 1417 (s), 1346 (s), 1285 (m), 1245 (s), 1189 (m), 1132 (w), 1060 (m), 986 (w), 951 (m), 852 (w), 813 (m), 708 (m), 619 (w), 557 (w), 434 (w).

The synthesis of complexes **2**−**8** were the same as that for **1** except that the $Ce(Cl)_3·6H_2O$ was replaced by other $LnCl_3·6H_2O$.

**Synthesis of [Nd(cpia)(H$_2$O)$_2$]·4H$_2$O (2).** Yield: 37.9% based on Nd. Elemental analysis (%) calcd for $C_{12}H_{22}NdNO_{13}$ (532.6): C 27.06, H 4.16, N 2.63; found: C 27.22, H 4.05, N 2.70. IR (KBr pellet, cm$^{-1}$): 3388 (s), 2909 (w), 1613 (s), 1577 (s), 1521 (s), 1463 (s), 1423 (s), 1345 (m), 1273 (m), 1239 (s), 1191 (m), 1136 (w), 1070 (m), 982 (m), 950 (m), 852 (w), 806 (m), 721 (m), 606 (w), 429 (w).

**Synthesis of [Sm(cpia)(H$_2$O)$_2$]·4H$_2$O (3).** Yield: 42.2% based on Sm. Elemental analysis (%) calcd for $C_{12}H_{22}SmNO_{13}$ (538.7): C 26.76, H 4.11, N 2.60; found: C 26.92, H 3.99, N 2.66. IR (KBr pellet, cm$^{-1}$): 3404 (m), 2908 (w), 1623 (m), 1573 (s), 1522 (m), 1463 (m), 1428 (s), 1330 (w), 1273 (w), 1241 (s), 1189 (w), 1137 (w), 1070 (m), 983 (w), 951 (w), 852 (w), 805 (w), 724 (w), 695 (w), 604 (w).

**Synthesis of [Eu(cpia)(H$_2$O)$_5$]$_2$·2H$_2$O (4).** Yield: 39.0% based on Eu. Elemental analysis (%) calcd. for $C_{24}H_{44}Eu_2N_2O_{26}$ (1080.5): C 26.67, H 4.10, N 2.59; found: C 26.74, H 3.98, N 2.63. IR (KBr pellet, cm$^{-1}$): 3425 (s), 2898 (w), 1643 (s), 1592 (s), 1544 (s), 1455 (s), 1434 (s), 1346 (m), 1232 (m), 1170 (m), 1070 (m), 977 (w), 930 (w), 850 (w), 809 (w), 701 (m), 679 (w), 525 (w).


dx.doi.org/10.1021/cg400174r | Cryst. Growth Des. 2013, 13, 3374−3380

**Synthesis of [Gd(cpia)($H_2O$)$_5$]$_2$·2$H_2O$ (5).** Yield: 46.5% based on Gd. Elemental analysis (%) calcd. for $C_{24}H_{44}Gd_2N_2O_{26}$ (1091.1): C 26.42, H 4.06, N 2.57; found: C 26.55, H 3.92, N 2.64. IR (KBr pellet, $cm^{-1}$): 3438 (s), 2902 (w), 1639 (s), 1589 (s), 1510 (s), 1453 (m), 1432 (m), 1409 (m), 1347 (w), 1233 (w), 1192 (w) 1072 (w), 977 (w), 928 (w), 813 (w), 680 (w), 570 (w), 528 (w).

**Synthesis of [Tb(cpia)($H_2O$)$_5$]$_2$·2$H_2O$ (6).** Yield: 37.8% based on Tb. Elemental analysis (%) calcd. for $C_{24}H_{44}Tb_2N_2O_{26}$ (1094.5): C 26.34, H 4.05, N 2.56; found: C 26.51, H 3.94, N 2.60. IR (KBr pellet, $cm^{-1}$): 3426 (s), 2900 (w), 1639 (s), 1511 (s), 1450 (m), 1431 (s), 1409 (s), 1345 (m), 1232 (w), 1075 (m), 980 (w), 930 (w), 847 (w), 810 (m), 724 (w), 692 (w), 569 (w), 531 (w).

**Synthesis of [Er(cpia)($H_2O$)$_5$]$_2$·2$H_2O$ (7).** Yield: 43.7% based on Er. Elemental analysis (%) calcd. for $C_{24}H_{44}Er_2N_2O_{26}$ (1111.1): C 25.94, H 3.99, N 2.52; found: C 26.02, H 3.85, N 2.57. IR (KBr pellet, $cm^{-1}$): 3436 (m), 2888 (w), 1680 (m), 1646 (s), 1551 (m), 1517 (m), 1456 (m), 1436 (s), 1334 (w), 1283 (w), 1261 (w), 1176 (wm), 1131 (w), 1078 (m), 981 (w), 935 (w), 851 (w), 809 (w), 714 (m), 636 (w), 697 (w), 525 (w).

**Synthesis of [Lu(cpia)($H_2O$)$_4$]$_2$·2$H_2O$ (8).** Yield: 41.2% based on Lu. Elemental analysis (%) calcd. for $C_{24}H_{40}Lu_2N_2O_{24}$ (1090.5): C 26.43, H 3.70, N 2.57; found: C 26.59, H 3.64, N 2.63. IR (KBr pellet, $cm^{-1}$): 3638 (m), 3301 (m), 2380 (w), 1597 (s), 1510 (m), 1441 (m), 1397 (m), 1345 (m), 1232 (m), 1189 (w), 1154 (w), 1067 (w), 928 (w), 815 (w), 684 (w), 519 (w).

**X-ray Crystallography.** Single-crystal X-ray diffraction data for complexes **1**−**8** were collected on a Rigaku R-AXIS RAPID imaging plate diffractometer with graphite-monochromated Mo K$\alpha$ ($\lambda$ = 0.71073 Å) at 291 K. Empirical absorption corrections based on equivalent reflections were applied. The structures of **1**−**8** were solved by direct methods and refined by full-matrix least-squares methods on $F^2$ using the SHELXS-97 crystallographic software package.[15] One of the lattice water molecules was free-refined isotropically and was disordered over two positions with an occupancy of 0.34 and 0.66 in **1**, 0.38 and 0.62 in **2**, 0.37 and 0.63 in **3**, and their H atoms were not added. The crystal parameters, data collection, and refinement results for **1**−**8** are summarized in Table 1. Selected bond lengths are listed in Table S1 (see the Supporting Information).

## RESULTS AND DISCUSSION

**Synthesis.** The crystals of complexes **1**−**8** were synthesized by using solution diffusion reactions rather than the hydrothermal reactions, which is normally applied in the reactions of organic acids and metal ions. In the preparation of complexes **1**−**8**, a 3 mL water solution was used as a buffer layer to reduce the output of powder. Such a process improves the yield and purity of the crystal products. Furthermore, the influence of the counteranions was investigated by employing the lanthanide nitrates instead of lanthanide chlorides. However, the same products were obtained with slight difference in the yields. Notably, the reaction temperature affects the structure of complexes **1**−**3**. When the reaction temperature was above 25 °C, complexes **1**−**3** were isolated. When the reaction temperature was below 25 °C, complexes **1**−**3** were not isolated. However, complexes **4**−**8** were able to be isolated easily by mixing the $Na_3$(cpia) ligand and lanthanide salts in $H_2O$. In fact, the yields for complexes **1**−**8** are based on the crystalline products. The overall yields including the powder product for complexes **4**−**8** are quite high. However, the yields for complexes **1**−**3** were low because some unknown byproduct remained. Complexes **1**−**8** were heated at 80 °C under a vacuum for 2 h to obtain the dehydrated products, namely, complexes **1′**−**8′**.

**Crystal Structure of Complexes 1−3.** Single-crystal X-ray diffraction analysis shows that complexes **1**−**3** are isomorphic. In a typical structure of **1**−**3**, complex **1** crystallizes in the triclinic system with $P\bar{1}$ space group. The asymmetric unit of **1** has one Ce(III) cation, one cpia$^{3-}$ anion, two coordinated water molecules, and four lattice water molecules (Figure 1a). The Ce(III) cation is nine-coordinated in a tricapped triangular prism geometry defined by seven O atoms from six carboxyl groups of five cpia$^{3-}$ anions and two O atoms from two coordinated water molecules. The bond distances around the Ce1 center are in range of 2.431(2)−2.627(3) Å. The cpia$^{3-}$ anions serve as a hexadentate ligand coordinating with five Ce(III) cations involving all of three carboxylate groups in binding mode of $\mu_5$ - $\eta^1$: $\eta^1$: $\eta^1$: $\eta^1$: $\eta^2$: $\eta^1$. The three carboxylate groups exhibit different coordination modes: (a) the carboxylate group from hydroxyacetic acid group shows bridging coordination mode, which link two Ce(III) cations to form a dinuclear {$Ce_2$} moiety with a Ce···Ce distance of 4.127(1) Å; (b) one carboxylate group of the iminodiacetic acid group exhibits chelating and bridging mode coordinating with one dinuclear {$Ce_2$} moiety; (c) the other one shows the bridging mode linking two dinuclear {$Ce_2$} moieties (Scheme 1).

**Scheme 1. Coordination Modes of cpia$^{3-}$ Anions in Complexes 1−8**

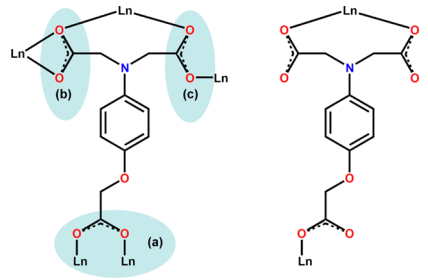


in complexes **1**–**3** in complexes **4**–**8**

Through these coordinated interactions, a double chain is built up by cpia$^{3-}$ anions linking the Ce(III) cations with the distance between two {$Ce_2$} moieties of 12.086(6) Å along the [0 1 $\bar{1}$] direction. Furthermore, the adjacent double chains are connected by a third coordinated mode to form a two-dimensional (2D) double layer structure with the lattice water molecules filling in the cavities with a dimension of 5.575(1) × 12.608(5) Å and stabilizing by the hydrogen bonds (Figure 1b). Adjacent networks are in an A−B type offset fashion and linked by O−H···O hydrogen bonds between coordinated and lattice water molecules into a 3D supramolecular framework (Figure 1c, hydrogen bond distances and angles; see Table S2).

**Crystal Structure of Complexes 4−8.** Complexes **4**−**8** crystallize in the monoclinic system with $C2/c$ space group and are also isomorphic. In a typical structure of **4**−**8**, the asymmetric unit of complex **4** consists of one Eu(III) cation, one cpca$^{3-}$ ligand, five coordinated water molecules, and one lattice water molecule (Figure 2a). The Eu(III) cation is eight-coordinated in a distorted square antiprismatic geometry defined by two O atoms from two carboxylate groups of one cpia$^{3-}$ anion, one O atom from another cpia$^{3-}$ anion, and five O atoms from five coordinated water molecules. The bond distances of Eu−O range from 2.257(2) to 2.453(3) Å. The three carboxylate groups of the cpia$^{3-}$ anion in complex **4** are monodentate coordinations ($\mu_2$ - $\eta^1$: $\eta^0$: $\eta^1$: $\eta^0$: $\eta^1$: $\eta^0$) with adjacent Eu(III) cations (Scheme 1) to construct a [2 + 2] rectangle metallomacrocycle. Each [2 + 2] metallomacrocycle is surrounded by eight other metallomacrocycles (Figure 2b). Furthermore, these metallomacrocycles and lattice molecules


dx.doi.org/10.1021/cg400174r | Cryst. Growth Des. 2013, 13, 3374−3380

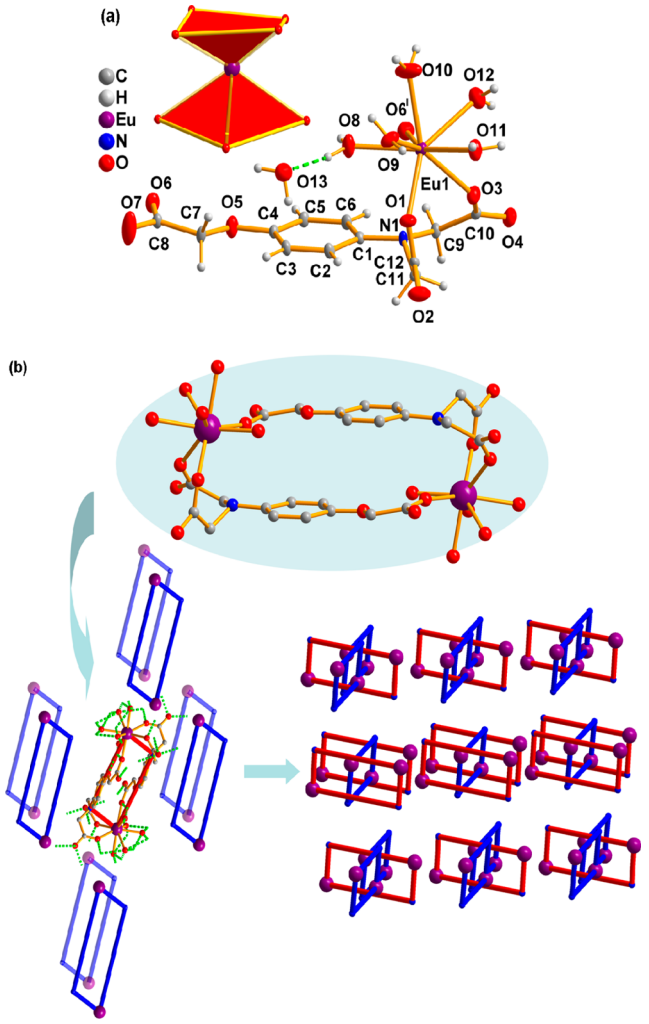


**Figure 2.** (a) Stick-ellipsoid representation of the asymmetric unit of complex **4** with thermal ellipsoids at 50% probability. The inset shows the coordination geometry of the Eu(III) center; (b) schematic illustration of 3D stacking framework. Symmetry codes: (I) $-x$, $1-y$, $-z$.

are linked together through O−H···O hydrogen bonds to form a 3D supramolecular framework with the adjacent layers consisting of the [2 + 2] metallomacrocycles with different orientations (Figure 2c, Table S2).

However, in complex **8**, the Lu(III) cation is seven-coordinated in a distorted monocapped triangular prism geometry due to the lanthanide contraction causing only four water molecules coordination with the Lu(III) cation (Figure S1, Supporting Information). According to the order of the lanthanide contraction, the bond distances of Ln−O and Ln···Ln decrease linearly in **1**−**3** and **4**−**8**, respectively. The coordination numbers for the lanthanide ions are also declined from 9 to 7 in complexes **1**−**8** (Figure 3). Notably, the structural differences between the complexes **1**−**3** and **4**−**8** should be caused by the combined effect of the lanthanide contraction and the thermodynamics effect.

**PXRD and Thermalgravimetric Analysis.** The PXRD patterns for complexes **1**−**8** and complexes **1′**−**8′** are presented in Figure S2. The diffraction peaks of both calculated and experimental patterns match well, indicating the phase purities of complexes **1**−**8**. The diffraction peaks of the complexes **1′**−**3′** show an absence of the peaks around 10°, which may be

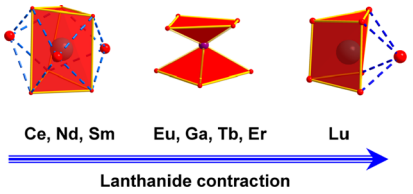


**Figure 3.** Coordination geometry changes of the lanthanide centers in complexes **1**−**8**.

caused by the partial collapse of the framework. However, the diffraction peaks of the complexes **4′**−**8′** exhibit an additional peak near 7.7° in contrast to those for complexes **1**−**8**, which may indicate the change of the molecules packing. The TGA measurements of complexes **1**−**8** were carried out in atmosphere in the temperature range 30−800 °C (Figure S3). Complexes **1**−**3** exhibit similar two weight-loss processes. The first weight loss of 11.82% for **1**, 14.05% for **2**, and 12.28% for **3**, respectively, correspond to the loss of four lattice water molecules per formula unit (calcd: 13.62% for **1**, 13.52% for **2**, and 13.37% for **3**) in the temperature range of 30−115 °C. The frameworks of complexes **1**−**3** collapse near 295 °C arising from the decomposition of the $cpia^{3-}$ anions and coordinated water molecules. The observed final mass residue of 32.04%, 31.48% and 33.95%, respectively, likely are ascribed to generation of corresponding $Ln_2O_3$ (calcd: 31.06% for **1**, 31.59% for **2** and 32.38% for **3**). The TGA curves for complexes **4**−**8** also show similar two weight loss processes. The first weight loss of 19.29% for **4**, 19.61% for **5**, 19.74% for **6**, 18.94% for **7**, and 16.51% for **8**, respectively, was observed in the range of 80−180 °C, which corresponds to the loss of 12 lattice water molecules (10 lattice water molecules for **8**) per formula unit (calcd: 19.99% for **4**, 19.79% for **5**, 19.74% for **6**, 19.44% for **7**, and 15.59% for **8**). Furthermore, the second weight loss occurred in the temperature range of 310−700 °C, which corresponds to the loss of two $cpia^{3-}$ anions per formula unit. The observed final mass residue of 33.47%, 34.24%, 34.20%, 34.27%, and 37.55%, respectively, could be ascribed to the residue of corresponding $Ln_2O_3$ (calcd: 32.57% for **4**, 33.22% for **5**, 33.43% for **6**, 34.44% for **7**, and 37.55% for **8**).

**Luminescent Properties.** The UV−vis spectrum of the $H_3cpia$ is recorded in MeOH solution (Figure S4). The typical absorption at 264 nm is attributed to the $\pi-\pi^*$ transition of the aromatic rings. The peak at 320 nm is attributed to $n-\pi^*$ transition belonging to the tertiary amine group. The photoluminescence (PL) spectra of free $H_3cpia$, **4** and **6**, and the dehydrated complexes **4′** and **6′** were obtained in solid state at room temperature. Upon excitation at the characteristic absorbance band of the ligand $H_3cpia$ ($\lambda_{max}$ = 375 nm, Figure S5), solid samples of complexes **4** and **6** show the characterized visible luminescence of Eu(III) and Tb(III) ions at room temperature. As expected, complex **4** exhibits four characteristic emission bands of Eu(III) ion at 592, 614, 648, and 698 nm, respectively, which are attributed to the transition of $^5D_0 \rightarrow {}^7F_J$ (J: 1 to 4) (Figure 4a). The strongest peak at 614 nm from the $^5D_0 \rightarrow {}^7F_2$ transition results in red emission. Complex **6** exhibits four characteristic emission bands of Tb(III) ion at 490, 544, 586, and 620 nm, attributed to the transition of $^5D_4 \rightarrow {}^7F_J$ (J: 6 to 3) (Figure 4b). The strongest peak at 544 nm from the $^5D_4 \rightarrow {}^7F_5$ transition results in green light emission. Notably, the PL spectra for complexes Sm(III) (**3**) and Er(III) (**7**) and their dehydrated species **3′** and **7′** were also obtained; however, the characterized peaks for both Er(III) and Sm(III)


dx.doi.org/10.1021/cg400174r | Cryst. Growth Des. 2013, 13, 3374−3380

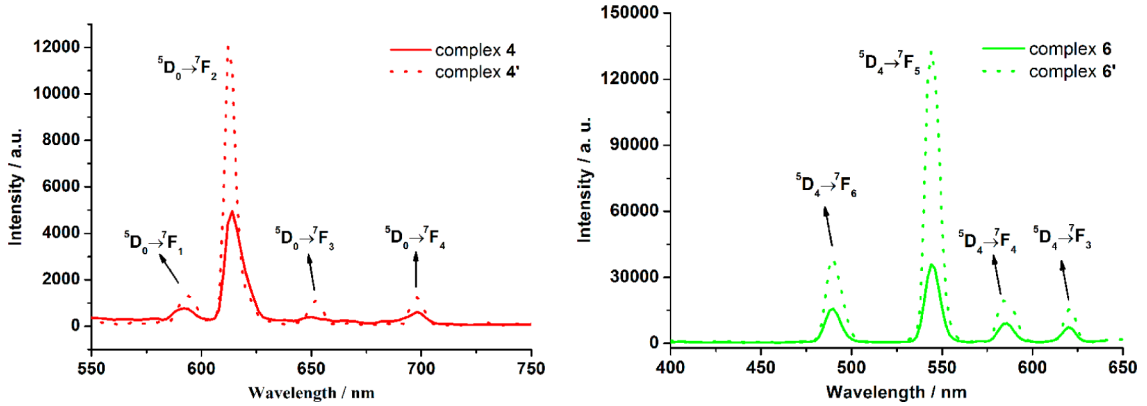


**Figure 4.** Solid-state emission spectra of complexes **4**, **4′**, **6**, and **6′**.

ions were not observed, which should be caused by the poor sensitization efficiency of the ligand for the Er(III) and Sm(III) ions.

The room-temperature luminescent decay profiles (Figure S6) of complexes **4** and **6** are found to be single-exponential functions, thus implying the presence of only one emissive Eu(III) or Tb(III) center, respectively. The lifetimes of 101.9 and 197.1 $\mu$s were determined by monitoring the emission decay curves within the $^5D_0 \rightarrow {}^7F_2$ transition at 614 nm for **4**, and $^5D_4 \rightarrow {}^7F_5$ transition at 544 nm for **6**. Noticeably, the intensity of the emissions for the dehydrated complexes **4′** and **6′** both show significant enhancements. And the lifetimes increase up to 283.3 $\mu$s for complex **4′** and 621.3 $\mu$s for complex **6′**.

**NIR Luminescence.** The NIR luminescent spectrum of the solid state complex **2** was investigated at room temperature. For complex **2**, upon excitation at 323 nm (Figure 5), the broad

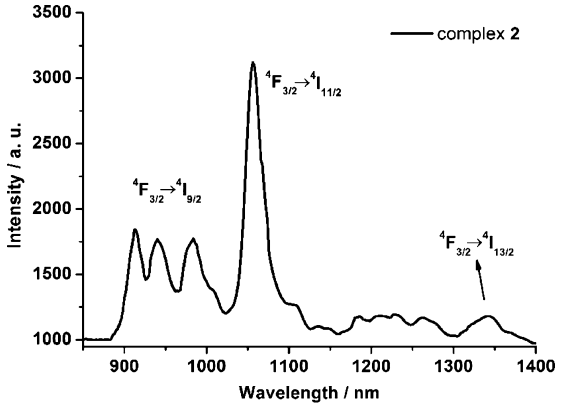


**Figure 5.** Solid-state NIR emission spectrum of complex **2**.

emission band with triple peaks in the range of 900−990 nm is observed and assigned to $^4F_{3/2} \rightarrow {}^4I_{9/2}$ transition. The strongest emission band occurring at 1056 nm is assigned to $^4F_{3/2} \rightarrow {}^4I_{11/2}$ transition; moreover, the emission band at 1344 nm is assigned to $^4F_{3/2} \rightarrow {}^4I_{13/2}$ transition, which offers the opportunity to develop new laser and optical amplified materials.[16−18]

**Energy Transfer.** To demonstrate the energy transfer process, the phosphorescence spectrum of complex **5** was measured at 77 K in a mixed solution of methanol/DMF (4:1 V/V) with a concentration of $1 \times 10^{-4}$ mol·L$^{-1}$. On the basis of the phosphorescence spectrum of complex **5** (Figure S7), the 0−0 transition is the band at 404 nm (24 752 cm$^{-1}$). Since the lowest excited state, $^6P_{7/2}$, of the Gd(III) ion is too high to accept energy from the ligand, the data obtained from the phosphorescence spectrum actually reveal the triplet energy level of cpia$^{3-}$ anion in lanthanide complexes.[19] According to Dexter's theory,[20] the suitability of the energy gap between the resonance level of the Ln(III) ion and the triplet state of the ligand is a critical factor for efficient energy transfer. If the energy gap is too large, the energy transfer rate constant decreases due to the diminution in the overlap between the donor and the acceptor. On the contrary, if the energy gap is too small, the energy back-transfer can occur from the Ln(III) ion to the resonance level of the triplet state of the ligand. Latva's empirical rule states that an optimal ligand-to-metal energy transfer process needs $\Delta E$ ($^3\pi\pi^* - {}^5D_J$) = 2500−4000 cm$^{-1}$ for Eu(III) and 2500−4500 cm$^{-1}$ for Tb(III) ions.[21] The triplet levels of the cpia$^{3-}$ anion (24 752 cm$^{-1}$) are obviously higher than the $^5D_0$ and $^5D_4$ levels of Eu(III) (17 500 cm$^{-1}$) and Tb(III) (20 400 cm$^{-1}$), and their energy gaps $\Delta E$ ($^3\pi\pi^* - {}^5D_0/{}^5D_4$) are 7252 and 4352 cm$^{-1}$, respectively (Figure 6). It supports the observation of stronger emission of the Tb(III) ion in complex **6** than that of Eu(III) ion in complex **4**.

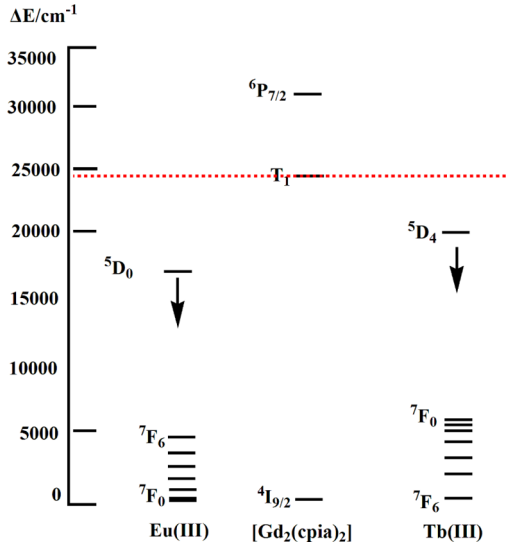


**Figure 6.** Simplified energy diagram showing the lowest lanthanide excited and the estimated states triplet state of the sensitizer cipa$^{3-}$ anion in the [$Gd_2$(cpia)$_2$] complex.


dx.doi.org/10.1021/cg400174r | *Cryst. Growth Des.* 2013, 13, 3374−3380

## CONCLUSION

Two series of eight polycarboxylate lanthanide coordination complexes, constructed by $cpia^{3-}$ anions and lanthanides featuring a unique 2D double layer and [2 + 2] rectangle metallomacrocycle structures, have been isolated, which represent the first examples of LMOCs based on $H_3cpia$. Isolation of complexes **1**−**8** unambiguously demonstrates that the lanthanum contraction dominates the structures of these complexes. PL spectra reveal that $cpia^{3-}$ anions are able to sensitize the luminescence of Nd(III), Eu(III), and Tb(III) ions in complexes **2**, **4**, and **6**, respectively. The study on the energy transfer between the resonance level of the Ln(III) ion and the triplet state of the ligand suggests that the match of the energy gap for complex **6** is better than that for complex **4**, resulting in the strong green luminescence for complex **6**. Further, both luminescent intensity and lifetimes for the dehydrated complexes **4′** and **6′** are significantly enhanced in contrast to those for complexes **4** and **6**. This approach offers the opportunity to develop potential laser and optical amplified materials.

## ASSOCIATED CONTENT

### Supporting Information

Tables S1−S2 and Figures S1−S6. This material is available free of charge via the Internet at http://pubs.acs.org. Crystallography data have been deposited to the Cambridge Crystallography Data Centre with deposition numbers CCDC nos. 909631−909634, 921245, 909635, 909636, and 919816 for complexes **1**−**8**.

## AUTHOR INFORMATION


### Corresponding Author

*(G.M.L.) Tel.: +86 451 86608458; fax: +86 451 86673647; e-mail: gmli_2000@163.com. (P.-F.Y) e-mail: yanpf@vip.sina.com.


### Notes

The authors declare no competing financial interest.

## ACKNOWLEDGMENTS

This work is financially supported by the National Natural Science Foundation of China (Nos. 21072049, 21072050, 21272061), Heilongjiang Province (No. 2010td03), and Heilongjiang University (2010hdtd-08 and 2010hdtd-11).

## REFERENCES


(1) (a) Eddaoudi, M.; Kim, J.; Rosi, N.; Vodak, D.; Wachter, J.; O'Keeffe, M.; Yaghi, O. M. *Senience* **2002**, *295*, 469. (b) Matsuda, R.; Kitaura, R.; Kitagawa, S.; Kubota, Y.; Belosludov, R. V.; Kobayashi, T. C.; Sakamoto, H.; Chiba, T.; Takata, M.; Kawazoe, Y.; Mita, Y. *Nature* **2005**, *436*, 238. (c) Ma, L. O.; Jin, A.; Xie, Z. G.; Lin, W. B. *Angew. Chem., Int. Ed.* **2009**, *48*, 9905.

(2) (a) Li, J. R.; Kuppler, R. J.; Zhou, H. C. *Chem. Soc. Rev.* **2009**, *38*, 1477. (b) Corma, A.; García, H.; Llabrés i Xamena, F. X. *Chem. Rev.* **2010**, *110*, 4606. (c) O'Keeffe, M.; Peskov, M. A.; Ramsden, S. J.; Yaghi, O. M. *Acc. Chem. Res.* **2008**, *41*, 1782.

(3) (a) Hou, G. F.; Bi, L. H.; Li, B.; Wu, L. X. *Inorg. Chem.* **2010**, *49*, 6474. (b) Hou, G. F.; Bi, L. H.; Li, B.; Wang, B.; Wu, L. X. *CrystEngComm* **2011**, *13*, 3526. (c) Hou, G. F.; Wang, X. D.; Yu, Y. H.; Gao, J. S.; Wen, B.; Yan, P. F. *CrystEngComm* **2013**, *15*, 249.

(4) (a) Liu, Y.; Eubank, J. F.; Cairns, A. J.; Eckert, J.; Kravtsov, V. C.; Luebke, R.; Eddaoudi, M. *Angew. Chem., Int. Ed.* **2007**, *119*, 3342. (b) Kitagawa, S.; Matsuda, R. *Coord. Chem. Rev.* **2007**, *251*, 2490. (c) Mulfort, K. L.; Hupp, J. T. *J. Am. Chem. Soc.* **2007**, *129*, 9604.

(5) (a) Bünzli, J. C. G.; Piguet, C. *Chem. Sov. Rev.* **2005**, *34*, 1048. (b) Bünzli, J. C. G. *Chem. Rev.* **2010**, *110*, 2729. (c) Eliseeva, S. V.; Bünzli, J. C. G. *Chem. Sov. Rev.* **2010**, *39*, 189. (d) Sabbatini, N.; Guardogi, M.; Lehn, J. M. *Coord. Chem. Rev.* **1993**, *123*, 201. (e) Kido, J.; Okamoto, Y. *Chem. Rev.* **2002**, *102*, 2357.

(6) (a) Archer, R. D.; Chen, H. Y.; Thompson, L. C. *Inorg. Chem.* **1998**, *37*, 2089. (b) Xu, J.; Cheng, J. W.; Su, W. P.; Hong, M. C. *Cryst. Growth Des.* **2011**, *11*, 2294. (c) Yan, X. H.; Li, Y. F.; Wang, Q.; Huang, X. G.; Zhang, Y.; Gao, C. J.; Liu, W. S.; Tang, Y.; Zhang, H. R.; Shao, Y. L. *Cryst. Growth Des.* **2011**, *11*, 4205. (d) Zhao, Y.; Jiao, C. Q.; Sun, Z. G.; Zhu, Y. Y.; Chen, K.; Wang, C. L.; Li, C.; Zheng, M. J.; Tian, H.; Sun, S. H.; Chu, W. *Cryst. Growth Des.* **2012**, *12*, 3191.

(7) Galaup, C.; Picard, C.; Cathala, B.; Cazaux, L.; Tisnes, P. *Helv. Chim. Acta* **1999**, *82*, 543.

(8) (a) Holz, R. C.; Thompson, L. C. *Inorg. Chem.* **1993**, *32*, 5251. (b) Li, J. Y.; Li, H. F.; Yan, P. F.; Chen, P.; Hou, G. F.; Li, G. M. *Inorg. Chem.* **2012**, *51*, 5050. (c) Li, H. F.; Yan, P. F.; Chen, P.; Wang, Y.; Xu, H.; Li, G. M. *Dalton Trans.* **2011**, *41*, 900.

(9) (a) Cao, R.; Sun, D. F.; Liang, Y. C.; Hong, M. C.; Tatsumi, K.; Shi, Q. *Inorg. Chem.* **2002**, *126*, 2087. (b) Zhang, H. B.; Li, N.; Tian, C. B.; Liu, T. F.; Du, F. L.; Lin, P.; Li, Z. H.; Du, S. W. *Cryst. Growth Des.* **2012**, *12*, 670. (c) Feng, R.; Jiang, F. L.; Wu, M. Y.; Chen, L.; Yan, C. F.; Hong, M. C. *Cryst. Growth Des.* **2010**, *10*, 2306. (d) Shi, P. F.; Chen, Z.; Xiong, G.; Shen, B.; Sun, J. Z.; Cheng, P.; Zhao, B. *Cryst. Growth Des.* **2012**, *12*, 5203.

(10) (a) Ghosh, S. K.; Bureekaew, S.; Kitagawa, S. *Angew. Chem., Int. Ed.* **2008**, *47*, 3403. (b) Zou, R. O.; Sakurai, H.; Xu, Q. *Angew. Chem., Int. Ed.* **2006**, *45*, 2542.

(11) (a) Zhang, A. J.; Wang, Y. W.; Dou, W.; Dong, M.; Zhang, Y. L.; Tang, Y.; Liu, W. S; Peng, Y. *Dalton Trans.* **2011**, *40*, 2844. (b) Zou, Y. H.; Wei, Q.; Guo, Z. L.; Chen, S. P.; Gao, S. L. *Inorg. Chim. Acta* **2011**, *375*, 181. (c) Li, Y. X.; Yan, P. F.; Hou, G. F.; Li, H. F.; Chen, P.; Li, G. M. *J. Organomet. Chem.* **2013**, *723*, 176.

(12) (a) Thomas, D.; Christian, S.; Nathalie, A.; Jerome, M.; Gerard, F. *J. Am. Chem. Soc.* **2005**, *127*, 12788. (b) Zhao, Y. H.; Xu, H. B.; Shao, K. Z.; Xing, Y.; Su, Z. M.; Ma, J. F. *Cryst. Growth Des.* **2007**, *7*, 513.

(13) Liu, C. B.; Wen, H. L.; Gong, Y. N.; Liu, X. M.; Tan, S. S. *Z. Anorg. Allg. Chem.* **2011**, *637*, 122.

(14) (a) Tan, S. S.; Wen, H. L.; Liu, C. B.; Peng, X. P. *Z. Kristallogr. NCS.* **2007**, *222*, 137. (b) Kaupp, G.; Naimi-Jamal, M. R.; Schmeyers, J. *Tetrahedron* **2003**, *59*, 3753.

(15) Sheldrick, G. M. *Acta Crystallogr. A* **2008**, *64*, 112.

(16) Klink, S. I.; Alink, P. O.; Grave, L.; Peters, F. G. A.; Hofstraat, J. W.; Geurts, F.; Van Veggel, F. C. J. M. *J. Chem. Soc., Perkin Trans.* **2001**, *63*, 363.

(17) Lai, W. P. W.; Wong, W. T. *New J. Chem.* **2000**, *24*, 943.

(18) Feng, J.; Yu, J. B.; Song, S. Y.; Sun, L. N.; Fan, W. Q.; Guo, X. M.; Dang, S.; Zhang, H. J. *Dalton Trans.* **2009**, 240.

(19) Wang, Y. W.; Zhang, Y. L.; Dou, W.; Zhang, A. J.; Qin, W. W.; Liu, W. S. *Dalton Trans.* **2010**, 9013.

(20) Dexter, D. L. *J. Chem. Phys.* **1953**, *21*, 836.

(21) Latva, M.; Takalo, H.; Mukkala, V. M.; Matachescu, C.; Rodriguez-Ubis, J. C.; Kankare, J. *J. Lumin.* **1997**, *75*, 149.